Pdfs of Paul Roesch's "Epigraphica", which were published in *Teiresias* from 1976 to 1986, are now available on application to the Editor. Please specify whether you prefer to have everything in one file or files for individual years.

WORK IN PROGRESS

121.0.01 Michael F. Lane, University of Maryland, Baltimore County (UMBC), sends the following report:

Archaeological Reconnaissance of Unexplored Remains of Agriculture (AROURA): Interim Report, 2010–2011 Campaigns

Michael F. Lane, University of Maryland, Baltimore County (UMBC) and Vassileios L. Aravantinos, 9th Ephorate of Prehistoric and Classical Antiquities (IX EPCA), Thebes

Summary, Methodology, and Theory

Archaeological Reconnaissance of Unexplored Remains of Agriculture, or "AROURA," is an official collaboration between the University of Maryland, Baltimore County, and the 9th Ephorate of Prehistoric and Classical Antiquities (IX EPCA), Thebes, Michael F. Lane and Vassileios L. Aravantinos respective Co-Directors. Athina Papadaki is the designated project Collaborator (Συνεργάτιδα) from the IX EPCA. Timothy J. Horsley (University of Michigan / Yale University) is the Principal Geophysical Investigator, assisted by Allison E. Cuneo (Boston University). Weston S. Bittner (UMBC) is the GIS Specialist. It has been funded by renewed research grants from the Institute for Aegean Prehistory.

The linchpin of AROURA, which began in the autumn of 2010, is extensive geophysical survey of the plain immediately around the Late Helladic IIIB fortress of Glas (Γλας), northern Boiotia, mainland Greece (**Figure 1**). Its aim is to detect traces of extensive agriculture of the kind recorded in the Linear B texts of several contemporary palace archives—that is, an agricultural strategy based on low human labor input and high animal labor and technological inputs, and reliance on a few modestly yielding, reliable crops (Halstead 1995, 2000). Its geophysical techniques are complemented by collection of finds from the ground surface, recovery of paleo-environmental remains, and methods to test geophysical results.

The fortress of Glas is found in the northeastern corner of the Kopaic Basin, once a bay of ancient Lake Kopaïs. (Classical descriptions of the Lake discussed in Kalcyk 1984; q.v. Ar.*Ach.*880ff., *Pax* 1005; *Il.*5.709; Livy 33.29.6; Pliny *N.H.*16.66.169; Plut.*Sulla* 20.2.4–5, *Pelop.*26.3; St.Byz. Ἀκραιφία, Κῶπαι; Str.9.2.40; Thphr.*H.P.*4.10). It sits within an ancient polder—that is, an area of land claimed from the waters and protected by a dike (**Figure 2**; Kenny 1935; Lauffer 1974, 1979). All previous and ongoing research and fieldwork indicate that the polder is contemporary with the inhabitation of the fortress (Iakovidis 1998; Lauffer 1986: 210–50). The polder is part of a system of drainage and irrigation works (**Figure 3**) dating to the same period, Late Helladic IIIB (c. 1300–1190 BCE) or possibly somewhat earlier, comprising much of the

northern and eastern edges of the Basin, and involving other polders (Iakovidis 2001: 149–57; Lauffer 1974, 1979; Spyropoulos 1971, 1973).

The Project Area of 1,018.44 hectares encompasses the polder and certain surrounding landforms and hydraulic features, and it is divided by a grid of 30-meter sampling squares (**Figure 4**), staked out as needed with differential GPS (global navigation satellite system, base station and rover). The area was selected because Glas is associated through architecture with the major palaces of the era (De Ridder 1894; Iakovidis 1998: 10–12; Wright 2005), and because it possesses stores of several thousand metric tons of one (less likely two) species of wheat (einkorn, *Triticum monococcum*), and probably olive oil too (Iakovidis 1998: 175; Jones 1995), evidence consistent with an extensive agricultural regime. Its setting of net deposition of alluvial sediment makes the conditions for preservation of remains of archaeological interest excellent compared with those surrounding other major Mycenaean sites (Aronis 1963; Mistardis 1967; Papadopoulos 1997; cf. Zangger et al. 1997), and this estimation seems to be confirmed by field marks—that is, crop and soil marks—in historic aerial photographs and recent satellite images (**Figure 5**; Knauss 1984: 213–7).

Dr. Lane, Co-Director, believes he can create plausible topographical models of the kind of landholding arrangements recorded in the Linear B archives. A starting point is early work of the late Emmett Bennett who noted the conformity of the order of land records in one textual series at Pylos (PY Eo–En) with two-dimensional space, and the probability therefore of contiguity or proximity among certain land plots (Bennett 1956). Lane relies too on the evident uniformity of absolute measures and equivalences of agricultural products in the widely scattered archives (De Fidio 1977: 81–9, 102–11; Lane, in press [2011]), including at Thebes 20 kilometers from Glas, and he makes additional inferences from agronomic and ethnographic sources to give topographical dimensions to areas under cultivation (Lane 2009). He has furthered hypothesized that the palace archives' surveillance of agriculture is not only partial, as many agree (Galaty and Parkinson 2007; Halstead 1992, 2007), but also limited to discrete, probably specially monitored and managed tracts of land close to or contiguous with each other (**Figure 6**; Lane, in press [2011]). He has also suggested that Glas is an instance of what is termed *wo-wo* or *wo-wi-ja* in Linear B, that is, a military fortress or garrison (cf. alphabetic Greek οὐρεῖον and φρούριον), constituting a node in a specialized logistical and communicational network, and hierarchy of command (Lane, in press [2012]).

Hence AROURA went into the field in 2010 with a set of expectations of what might or might not be encountered on or under the ground, as well as of the scale of sampling necessary. These include

- demarcated tracts of land tens and hundreds of meters in any dimension (**Figure 7**)
- rectilinear or near-rectilinear, built and excavated field partitions
- built or excavated remains of outbuildings for crop processing or temporary shelter
- pits for planting tree or vine crops, and
- plow scars in the subsoil from repeated plowing in one direction.

Appropriate techniques could therefore be applied. So far, geophysical prospection has been limited to magnetometry, because of its applicability anywhere contrast in magnetically susceptible iron oxides exists in soils. In particular, the Bartington 601-2 dual fluxgate gradiometer is employed because it collects data rapidly in pedestrian traverse and it can detect anomalies both near the surface and deeper than 1.5 meters (**Figure 8**). Critically, the magnetometric results are tested, or "ground-truthed," through cleaning and profiling of existing irrigation ditch sections (**Figure 9**) and soil coring (**Figure 10**), the latter with a permit from the Hellenic Institute of Geology and Mineral Exploration. Samples of soil from the cores are floated and wet-sieved. Selected land tracts are subject to collection of finds from their surface, and multispectral satellite data are analyzed for ranges that correlate with geophysical anomalies (**Figure 11**).

It became clear already in 2010 that the most archaeologically interesting magnetometry results could be distributed usefully among four categories. The first category comprises the area to the west of the polder dike (**Figure 12**), currently limited to Area H (**Figure 13**). This contains a network of magnetically positive anomalies, resembling a system of ditches filled with iron oxide-enhanced topsoil, a pattern observed in field marks too. The second includes the reticulate pattern of negative anomalies, east of the polder dike (**Figure 14**), typical of areas where topsoil or other traces of iron oxides have been removed, and these are also reflected in field marks. The constituent anomalies are oriented parallel and perpendicular to the dike, and they appear to be adjoined by narrower positive anomalies. Such pairing is typical of levees and accompanying ditches. The anomalies define near-squares, quadrilaterals between about 28 and 33 meters on a side. As of 2010, this pattern had been traced from Transect G1 into Transect I1, in the latter of which it broke down into a "herring bone" pattern of intervals closer to 15 meters in one dimension (**Figure 15**). The third category comprises the linear, net-negative, provisionally named "bounding" anomalies to the east of the reticulate pattern (**Figure 16**). These consist of long, apparently connected line segments, oriented from roughly north to south or northwest to southeast. They are generally wider than the elements of the reticulate pattern, though there are narrower bounding anomalies too. Above the southernmost of these detected in 2010 in G2, German investigators in the 1970s and 1980s found concentrations of limestone boulders, which they imagined could be remnant revetments of what they called the "Steindamm" (see Figure 2; Knauss 1987: 207–18). In the final category is the magnetically virtually empty zone right around the outcropping of Glas. The detection of discrete anomalies, some correlating with known features, such as the stone-lined canal running south-southwestward from Glas' eastern tip to Mt. Fteliá (**Figure 17**; Lauffer 1986: 210–50; Knauss 1984, 1987: 207–18), only accentuates the overall emptiness here. One recognizes immediately the absence of any evidence of an *Unterstadt*.

In 2011, the reticulate pattern was seen to continue into the northwest end of Transect I2, not sampled in 2010 (**Figure 18**). Together with Transect I1, to the northwest, and the southeast end of I2 (**Figure 19**), the results suggest that the pattern fades out as one progresses to the east. The pattern also appears to continue into Transect N1 further north (**Figure 20**), where it is unfortunately obscured by ferrous debris in the topsoil at the northwestern end. It seems again to become faint toward the east. It should be noted that the pattern of anomalies in N1 very closely shares orientation and interval with that in area Transect G1, where it is clearest.

Having just suggested that the reticulate pattern simply fades out to the east, results in 2011 nevertheless made clearer that the bounding anomalies do indeed mark its eastern limit, and that, conversely, the zone around Glas really is empty. For example, the long linear negative anomaly detected in the southeastern end of Transect I2 in 2010 can be seen to continue into Transect N2 (**Figure 21**) and from there into Transect J1 (**Figure 22**), where it seems to bifurcate (**Figure 23**), the western branch heading in the direction of the hill of Topólia, the northern terminus of the polder dike (see Figure 2). There is no trace of the pattern to the east of it.

Likewise, Transect A1 and Transect B3, both to the north of Glas, contain nothing like the pattern to the west. However, A1 contains a wide linear negative anomaly running nearly north to south through its eastern corner, with a narrower negative anomaly perhaps branching off to the west (**Figure 24**). This anomaly, which may again be paralleled by a narrower positive one, if pursued on the same alignment would intercept the Mycenaean canalization of the conjoined Kephissos and Melas Rivers to the north (Knauss 1984; Knauss 1987: 168–82), and the north scarp of Glas to the south (**Figure 25**).

Transect B3, within 100 meters of Glas' north gate, exhibits no anomaly typical of human constructions, though it does show large, relatively amorphous contrasts between positive and negative anomalies, typical of unevenness in the bedrock, and distinct spots of positive magnetic susceptibility, typical of infilled pits or areas of intense recent burning (**Figure 26**). It is from a horizon (c. 55–69 cm below grade) in a soil core from one of these "pit-like" anomalies, which contained degraded ceramic with a mixed fill (**Figure 27**), that AROURA obtained a sure AMS radiocarbon date from sediment of calibrated BC 5480–5370 (2 σ probability; Beta-301995).

The presence of the north–south anomaly in Transect A1 might raise the question of approaches to Glas, startlingly missing to some eyes. The revetted canal identified by our German predecessors, which runs from the Melas past Aghía Marína to the east end of Glas and onward to Fteliá, could have doubled as a causeway (see Figure 2). Satellite data suggest the existence of at least one suitable feature, running between Glas and the polder dike (**Figure 28**), though like the anomaly in Transect A1 and the revetted canal, it does not point directly at one of Glas' known gates. It may be reflected in a weak negative anomaly in Transect J3, referred to hereafter as a "connecting" anomaly, which appears to intersect a north–south bounding anomaly (**Figure 29**). Causeways to Glas may have deliberately been indirect, just as the empty zone may deliberately have been kept empty. Future exploration around the gates by Greek colleagues who have obtained the appropriate permissions will be most helpful.

Effects of Geological Substrate and Landform on Magnetometry

It is important to determine independently the nature and character of subsurface features corresponding to geophysical anomalies, because otherwise interpretation remains little more than conjecture. One should notice that the magnetic contrast in the results just presented is exceptionally low, generally within ±0.5 nanoTeslas (that is, 1.0 nT). At Plataiai in southern Boiotia, the contrast between on-site topsoil and limestone is about 7.0 nanoTeslas (Michael Boyd, pers. comm. 2010). However, the low contrast is expected of soils in the ancient lakebed, since they are largely minerogenic from a

calcareous substrate (Allen 1997: 47–8). The mass-specific magnetic susceptibility of the topsoil on Glas is about seven times that measured in a soil core taken from the Bay of Akraífnio, a few kilometers south of Glas (G. Tsokas, pers. comm. 2011; cf. Allen 1997: 41–2). Furthermore, there has been hardly a century of exposure of lake sediments in the 20th century CE that would allow soils, properly speaking, to form – about as little as there was in the 13th century BCE, the only other known period of effective drainage of the Basin's margins.

There is evidence of uneven ancient relief, contrasting with the modern plowed surface, which may account too for the attenuation of magnetic responses as one travels eastward from the reticulate pattern by the polder dike. For example, a band of particularly silt topsoil, first noted in 2010, runs from north to south past the west side of Glas, approximately between the reticulate pattern and the empty zone (**Figure 30**). This band of soils may be depicted in landscape paintings (e.g. Rottman 1839) as a strip of raised land occasionally emerging from the wetland margins. German investigators in the late 20th century concluded that there may have been seasonal passage on dry ground between Fteliá and Topólia in antiquity along a slight natural rise (Knauss, field notes 1984; Lauffer, unpub. report 1974), just as extant sections of the polder dike were used; they observed concentrations of, broadly speaking, Iron Age, pottery sherds near the western end of the mountain (Knauss, field notes 1984), just as AROURA observed sherds consistent with various periods—including Late Helladic, Geometric, Classical, and Medieval—apparently cast from the polder dike, at least to its west, toward the lake. There is also a rupestral inscription at the tip of Fteliá marking the boundary between Classical Akraiphia, to the southwest, and Kopai (Topólia) to the northeast (Jamot 1889; *SIG* 933).

It has occurred to us lately that the near coincidence of the bounding anomalies with this elevated strip may not be due to chance. If the bounding anomalies are somehow integral to the controlled drainage and irrigation of land in the polder, then they may have been strategically placed where the ground was mainly higher to achieve the desired effect with the help of gravity. For example, one plausible hypothesis is that the reticulate pattern to the east of the polder dike represents an ancient system of cultivated fields, such as is expected in the Mycenaean era, and that it was irrigated by a network of ditches fed from canals adjoining the bounding anomalies and ultimately from the canalized Kephissos–Melas to the north, which follows a natural rise a meter or two higher than the pattern. One may refer to the Lake Copais Company's map of the 1930s (**Figure 31**) to form a sense of the variation in relief just after modern drainage of the lake was finished. The Kephissos and the Melas would have flooded in the late autumn and early winter and again in the late winter and early spring, as they do today, and periodically more severely (*Paus*.9.38.6; Plut. *de gen.Socr*.578; Spon and Wheler 2004 [1678]: 305; Thphr.*C.P.*5.12.3, *H.P.*4.11.2), and this flooding would have been pronounced by their being constrained in leveed channels. Hence a further goal of AROURA is to clarify the regulatory mechanism of any irrigation, as well as that which let off any excess water from the fields (e.g. possibly through the dike and into Area H to the west). [Text continues Part B page 15: ed.]

1. Location of Glas in NE Kopaic Basin, with reference to Orkhomenos and Thebes (National Statistical Office of Greece 1:200,000-scale map of Boiotia / Viotía).

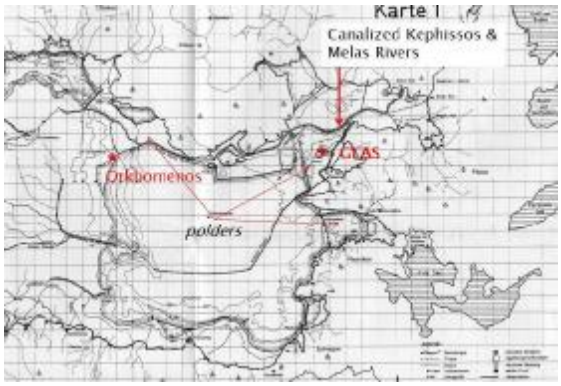

Fig. 2. System of LH III dikes, polders, canalized rivers, and flood-control dams in NE Kopais (after Knauss 1987,reproduced with author's permission

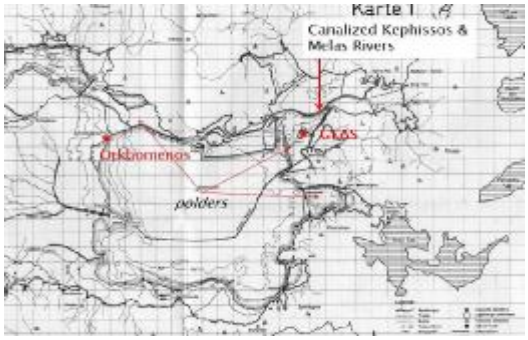

Fig. 3. LH III polders on N and E sides of Basin, with reference to Glas and Orkhomenos (after Knauss 1987, reproduced with author's permission).

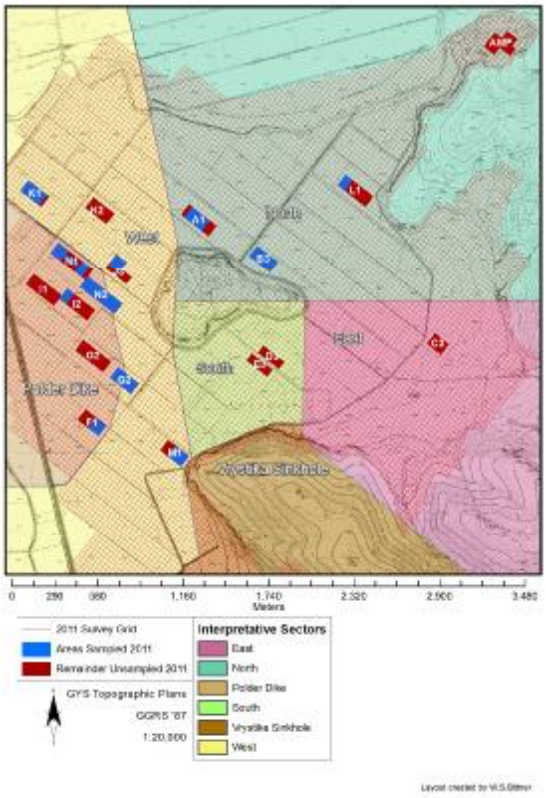

Fig. 4. Plan of AROURA Project Area / sampling grid in 2011, projected on Hellenic Military Geographic Service (HMGS) 1:5,000-scale topographic plan (base map).

Fig. 5. Orthorectified vertical aerial photograph of vicinity of Glas taken in October 1974, showing field marks mainly around polder dike to west (courtesy of J. Knauss; see also Kienast 1987).

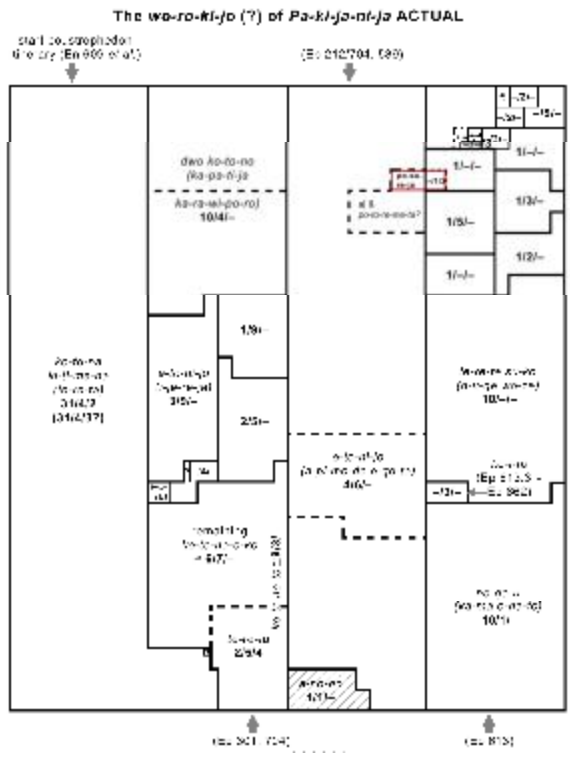

Fig. 6. Actual (v. "target") landholding arrangements at *pa-ki-ja-na,* based on analysis of Pylos Eb–Ep, Eo–En, and Ed series (from Lane, in press 2011; cf. Bennett 1956: 116).

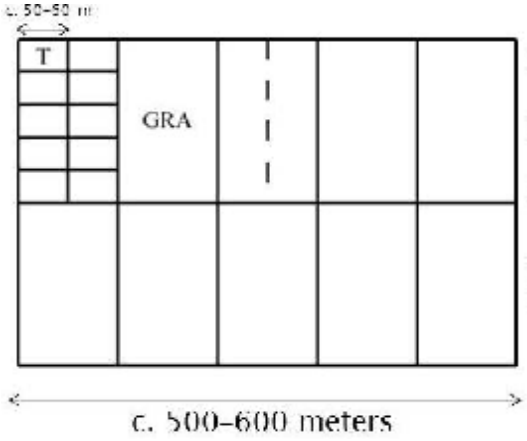

Fig. 7. One possible arrangement of Linear B land allocation units T and GRA (after Lane 2009).

.

Fig. 8. TJH employing Bartington 601-2

Fig. 9. Tapes and level lines set up for drawing profile of ditch section in Area I (M.F. Lane).

Fig. 10. Employment of soil auger in Area I. Soil has been placed stratigraphically in PVC tray in center. E.V. Iliopoulou is taking notes (M.F. Lane).

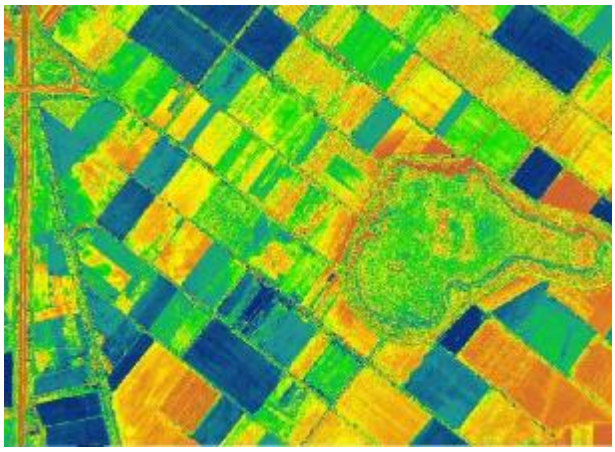

Fig. 11. Histogram-equalized near infrared band of eight-band multispectral Worldview-2 satellite data (dated October 2010).

Fig. 12. Cyclopean revetment on top of polder dike looking NNW toward Topólia / Kástro (ancient Kopai; M.F. Lane).

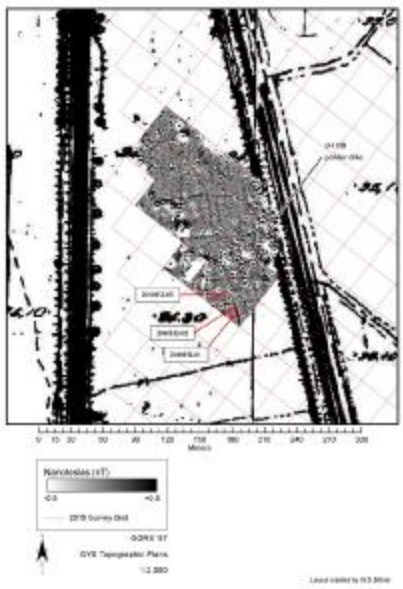

Fig. 13. AROURA magnetometry results in Area H (Transect H1 + Transect H2), projected on HMGS 1:5,000-scale topographic plan.

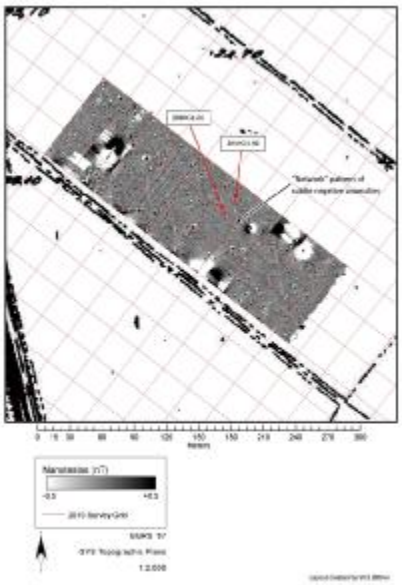

Fig. 14. AROURA magnetometery results in Transect G1, projected on HMGS 1:5,000-scale topographic plan.

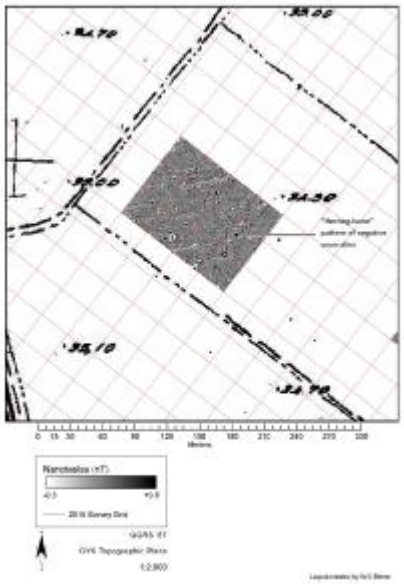

Fig. 15. AROURA magnetometry results in Transect I1, projected on HMGS 1:5,000-scale topographic plan.

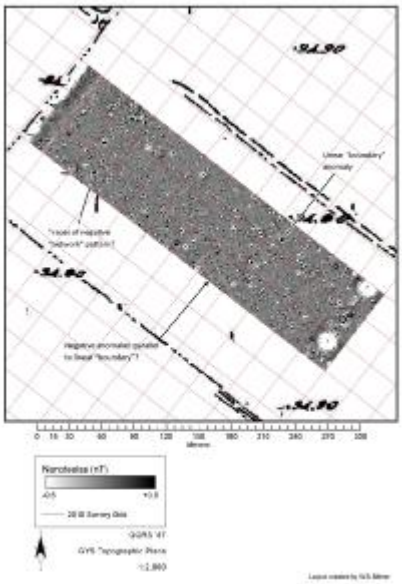

Fig. 16. AROURA magnetometry results in Transect G2, projected on HMGS 1:5,000-scale topographic plan.

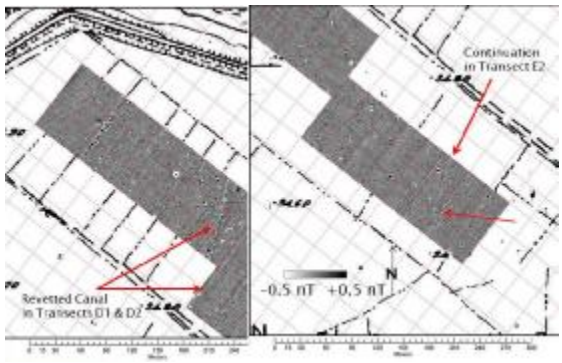

Fig. 17. Revetted canal evident in AROURA magnetometry results in Area D (Transect D1 + Transect D2), south of Glas' south gate (projected on HMGS 1:5,000-scale topographic plan).

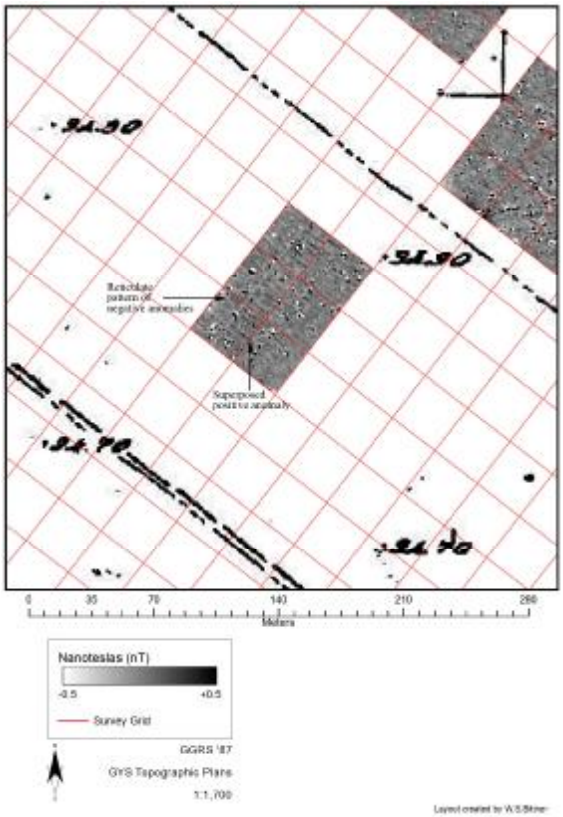

Fig. 18. AROURA magnetometry results in NW end of Transect I2, projected on HMGS 1:5,000-scale topographic plan

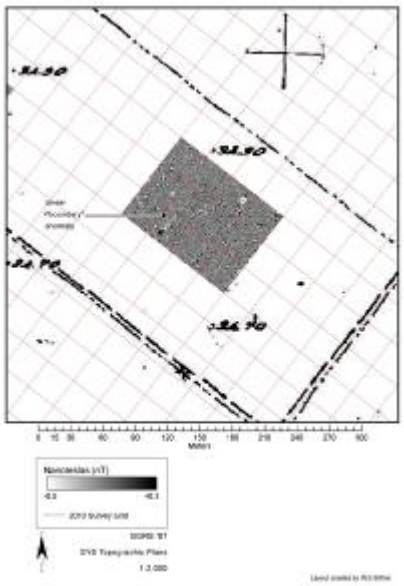

Fig. 19. AROURA magnetometry results in SE end of Transect I2, projected on HMGS 1:5,000-scale topographic plan.

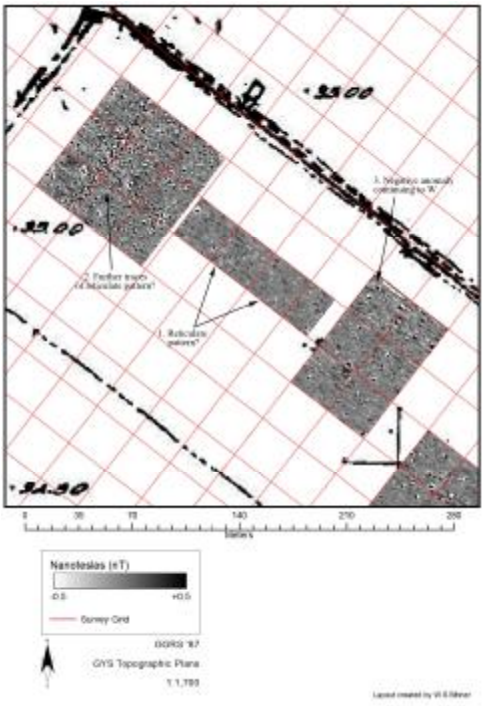

Fig. 20. AROURA magnetometry results in Transect N1, projected on HMGS 1:5,000-scale topographic plan.

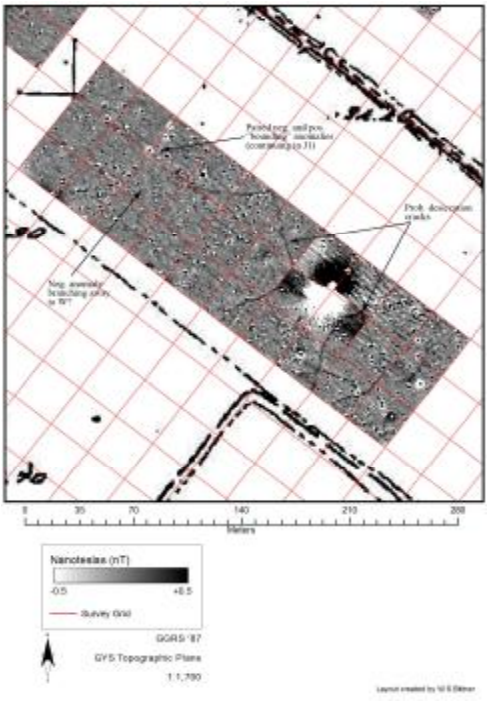

Fig. 21. AROURA magnetometry results in Transect N2, projected on HMGS 1:5,000-scale topographic plan.

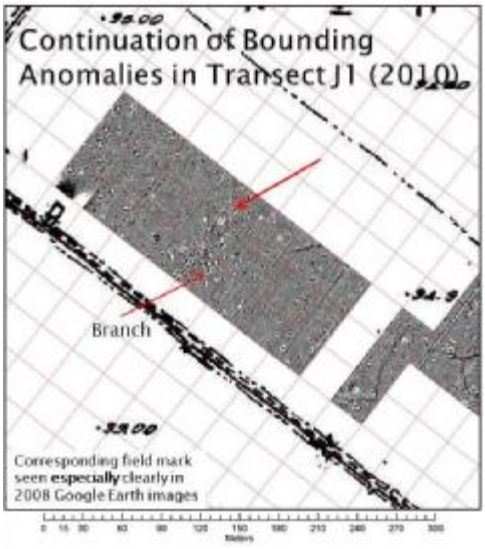

Fig. 22. AROURA magnetometry results in Transect J1, projected on HMGS 1:5,000-scale topographic plan.

Fig. 23. Google Earth composite satellite data (2008), showing bifurcation in field mark corresponding to bifurcation in "bounding" anomalies in Transect J1.

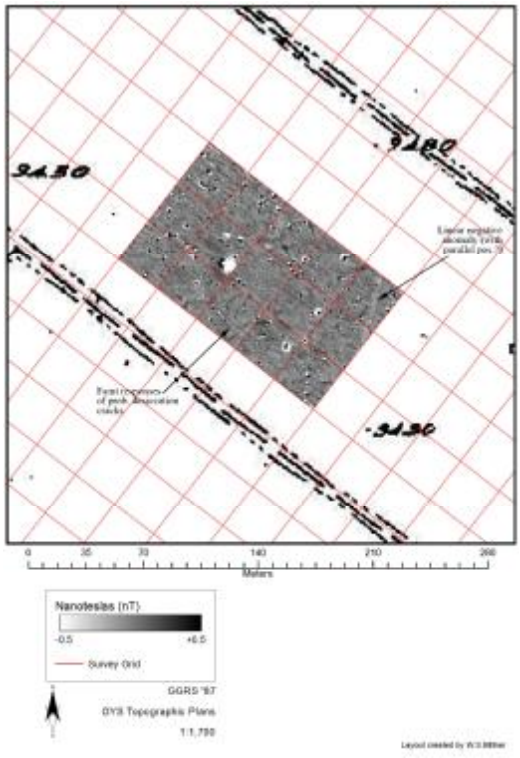

Fig. 24. AROURA magnetometry results in Transect A1, projected on HMGS 1:5,000-scale topographic plan.

Fig. 25. Alignment of N–S anomaly in Transect A1, showing its interception of the LH III channel of the Kephissos–Melas and the north scarp of Glas (projected on RGB composite Worldview-2 satellite image).

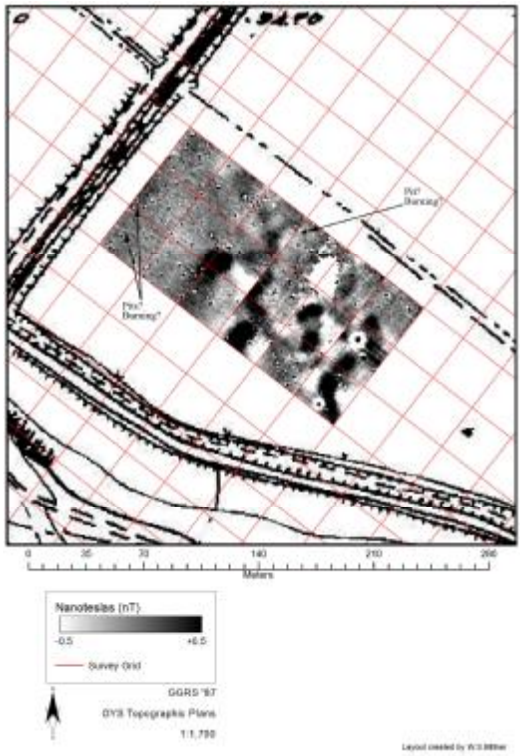

Fig. 26. AROURA magnetometry results in Transect B3, north of Glas' north gate, projected on HMGS 1:5,000-scale topographic plan.

Fig. 27. Soil core 2010B1-01, from a "pit-like" anomaly, showing probable degraded ceramic (5YR5/8 yellowish red) with mixed sandy fill (10YR4/2 dark gray, 10YR5/6 yellowish brown, and 10YR8/1 white).

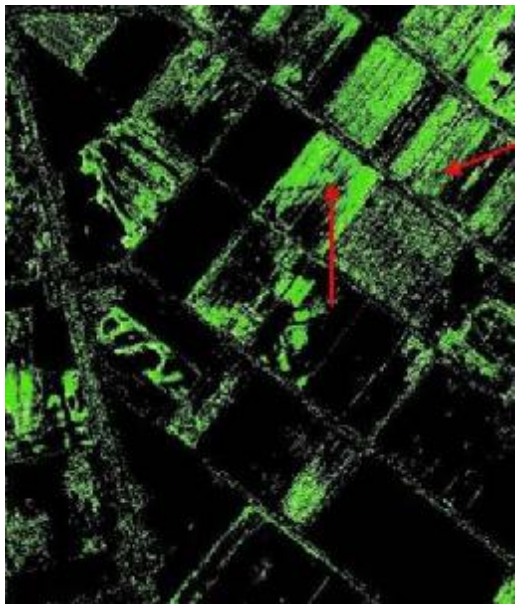

Fig. 28. Unsupervised reclassification of Worldview-2 band 8, near infrared 2, showing E–W field mark between Glas and polder dike.

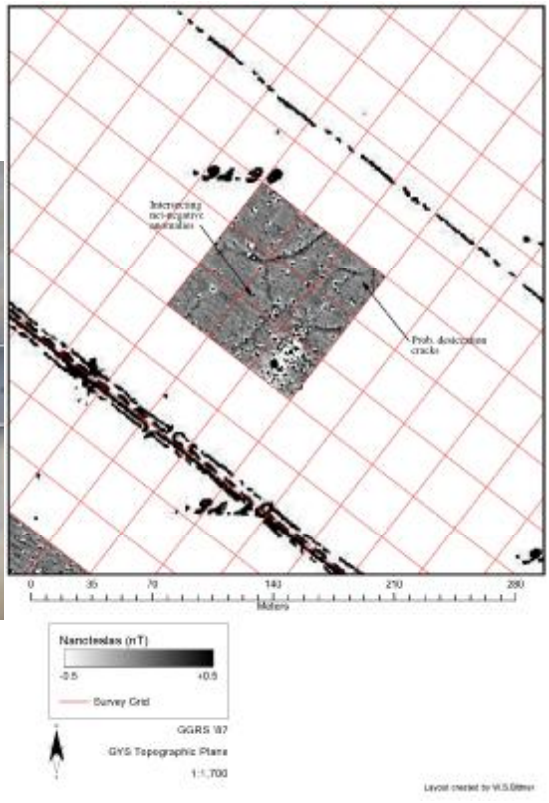

Fig. 29. AROURA magnetometry results in Transect J3, showing anomaly corresponding to E–W field mark, projected on HMGS 1:5,000-scale topographic plan

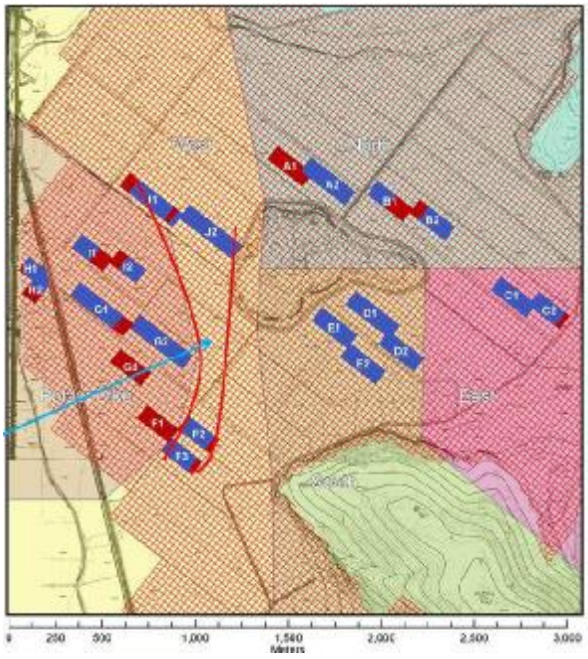

Fig. 30. Band of silty topsoil outlined in red approximately on plan of AROURA Project Area.

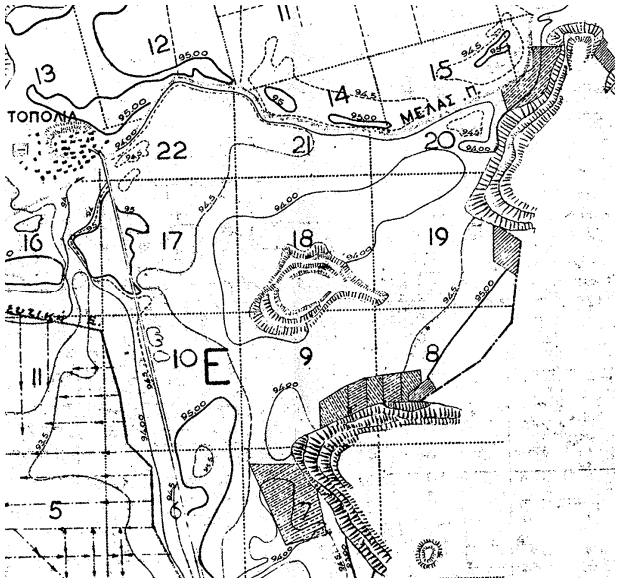

Fig. 31. Excerpt from Lake Copais Company 1:25,000-scale topographic map (n.d., c. 1931), showing relief around the outcropping of Glas varying between < 94 and > 95 meters a.m.s.l. (courtesy of J. Knauss).